

A Modular Demodulation System for Ultra-Weak Fiber Bragg Gratings

LUO Zhihui^{1,2}; LU Bo^{1,2}; XIANG Hao^{1,2}; YANG Zhen^{1,2}; XU Bing^{1,2*}

1. Hubei Engineering Research Center of Weak Magnetic-Field Detection, China Three Gorges University, Yichang 443002, China; 2. College of Science, China Three Gorges University, Yichang 443002, China

Abstract: To meet the requirements of field monitoring and deep system integration, this paper proposes, for the first time, a modular multi-channel demodulation system based on ultra-weak fiber Bragg gratings (UW-FBGs). The operating principle of the demodulation system is analyzed, and the relationships among spatial resolution, reflectivity and the number of gratings at the same wavelength are discussed. An embedded circuit is used to acquire and buffer 250 MSPS high-speed A/D data, while C# host software completes grating-array localization, wavelength analysis and data processing. Real-time demodulation of a four-channel sensing array is achieved. The system consumes less than 13 W, has dimensions of 230 mm x 170 mm x 40 mm, a spatial resolution of 2 m, a single-channel sensing distance greater than 10 km and more than 5,000 grating points, enabling large-scale sensing with UW-FBGs.

Keywords: ultra-weak fiber Bragg grating; wavelength demodulation; sensor; field-programmable gate array (FPGA); modularization

Figure and Table Captions

Fig. 1 UW-FBG demodulation system.

Fig. 2 UW-FBG demodulation module and circuit schematic.

Fig. 3 Interface of the UW-FBG demodulation device.

Fig. 4 Calibration of position information for a single-wavelength FBG array.

Fig. 5 Test results for a single-wavelength FBG array.

Fig. 6 Calibration of position information for a multi-wavelength FBG array.

Fig. 7 Test results for a multi-wavelength FBG array.

Fig. 8 Position calibration for four-channel FBG arrays.

Fig. 9 Test results for four-channel FBG arrays.

Fig. 10 Position and power calibration of the long-distance FBG array.

Fig. 11 Test results for the long-distance FBG array.

0. Introduction

Fiber Bragg grating (FBG) sensors feature high accuracy, good multiplexing capability, light weight, corrosion resistance and immunity to electromagnetic interference, and have been widely used in civil engineering and structural health monitoring. However, conventional FBGs have limited multiplexing capacity and complex fabrication processes, which makes them difficult to apply to large-capacity engineering monitoring. Ultra-weak fiber Bragg gratings (UW-FBGs) refer to grating sensors with reflectivity below 0.1%. Because of their extremely low reflectivity, the reflected optical powers of all grating points are nearly identical, allowing a large number of UW-FBG sensors with the same wavelength to be multiplexed on a single fiber and making large-capacity grating sensing networks possible.

As with conventional FBGs, UW-FBGs sense variations in external physical quantities by detecting shifts in Bragg wavelength. When thousands of UW-FBGs are distributed along one fiber, signal demodulation becomes a central issue for UW-FBG sensing networks. Previous studies have explored wavelength-scanning and time-domain localization, narrow-band filter conversion, wavelength-to-frequency transformation, hybrid ultra-wideband arrays and multi-wavelength interrogation. Application studies have also expanded into structural vibration identification, low-cost long-perimeter security, underground vertical strain monitoring and real-time landslide monitoring.

The development of low-power and miniaturized demodulation systems is critical for the wider application of UW-FBG technology. Existing rack-mounted systems, which combine low-level high-speed acquisition with X86 computer processing, are typically bulky and slow, consume more than 60 W and involve many interconnecting cables. This increases the failure rate and makes them difficult to use in field monitoring and deep system integration. A low-power and compact UW-FBG demodulation system is therefore urgently needed.

This paper proposes a modular UW-FBG demodulation system. The working principle is analyzed, and embedded circuitry is introduced to complete signal acquisition, processing and communication at the hardware level. The positions and wavelengths of UW-FBGs are demodulated in real time. By avoiding massive data upload and X86-based processing, the proposed system improves power consumption, demodulation speed and sensor capacity, providing a practical solution for large-scale sensing networks.

1. Operating Principle

The UW-FBG demodulation system consists of a demodulation module and a sensing grating array. The demodulation module includes a laser pulse generation unit, an optical path unit and a signal processing/control unit. The laser pulse generation unit contains a scanning laser with a wavelength range of 1528-1568 nm, a semiconductor optical amplifier (SOA) and an erbium-doped fiber amplifier (EDFA), and is used to generate optical pulses with variable wavelengths.

The optical path unit consists of a circulator, a four-channel optical switch and a photodetector, which complete optical-channel selection and optical-electrical conversion. The signal processing and control unit is built around a Xilinx Zynq7020 device that integrates an ARM processor and FPGA circuitry. It is responsible for human-machine interaction, initialization, data acquisition and processing.

During initialization, the signal processing/control unit sends commands to the laser pulse generation unit. The scanning laser emits continuous light, which is modulated by the SOA, amplified by the EDFA, routed through the circulator and selected optical channel, and then coupled into the UW-FBG array. The reflected light from the UW-FBGs is returned through the circulator and converted to electrical signals by the photodetector. The FPGA controls the A/D conversion circuit for high-speed acquisition and analysis to identify the grating positions. During measurement, the FPGA calculates the wavelength variation of each UW-FBG in real time based on the pre-determined grating positions. The ARM stores the results and transmits them to the host computer via USB or Ethernet.

The sensing grating array is primarily fabricated online on a draw tower using G.652D preforms. Time-division and wavelength-division multiplexing are supported. A single strengthened coating is adopted and the sliding layer of conventional fiber is removed, resulting in high tensile strength, low creep and good consistency.

The FPGA and RAM locate UW-FBGs according to the OTDR reflection principle. The distance from a grating point to the circulator is determined from the time at which the optical pulse reaches the grating and returns. The minimum resolvable distance between adjacent gratings depends on the pulse width and the delay between reflections. For a 20 ns optical pulse, the minimum grating spacing must be greater than 2 m.

In addition to spatial limitation, a shadowing effect exists among UW-FBGs. As the optical pulse propagates through the grating array, reflection loss from upstream gratings accumulates and gradually weakens the reflection from downstream gratings, causing spectral degradation. Multiple-reflection crosstalk may also occur. Studies show that when the reflectivity is lower than -35 dB, the influence of multiple reflections can be ignored. Considering the shadowing effect, the number of multiplexed gratings is approximately inversely proportional to the optimum reflectivity. Lower grating reflectivity enables more grating points to be multiplexed.

Based on these considerations, the system design uses gratings with low reflectivity to build the sensing array. The grating spacing is 2 m, the sensor count is 5,000 and the demodulation distance is 10 km.

2. Hardware and Software Design

The demodulation module integrates the laser pulse generation unit, optical path unit and signal processing/control unit inside an aluminum-machined enclosure, with an external fan. The module uses a 12 V DC power supply, consumes less than 13 W, has dimensions of 230 mm x 170 mm x 40 mm, and can operate stably at room temperature without starting the fan.

The hardware circuit is the key part of the UW-FBG demodulation module. It includes the Zynq7020 chip, peripheral circuits, A/D conversion circuits, optical pulse generation circuits, optical amplifier interface circuits, light source interface circuits, data upload circuits and power circuits. The A/D conversion circuit is the core. It includes signal conditioning and A/D conversion; the former converts single-ended analog signals into differential signals and amplifies them, while the latter converts analog signals into digital data.

Each A/D device supports two channels of 250 MSPS acquisition with 14-bit precision. Its output interface uses 16 LVDS differential pairs, including 14 data pairs, one overflow signal and one reference clock. The Zynq7020 circuit reads A/D data in real time, analyzes and processes the data matrix, extracts valid grating information and performs rapid spectral analysis. The board also integrates an optical pulse modulation circuit. Pulses generated inside the FPGA drive a high-speed switching chip, which modulates the continuous laser through the SOA to generate optical pulses. Pulse width and pulse period can be configured by the host computer.

The C# host demo software includes single-wavelength spectral display, real-time wavelength demodulation and a position-wavelength plot of the grating array. The single-wavelength spectrum display can show the spectrum of the selected grating by its serial number. The real-time wavelength demodulation interface displays the peak wavelength variation of the current grating. The position-wavelength plot shows the positions of all gratings in the fiber and the corresponding peak wavelength. For engineering measurement needs, parameter configuration, calibration, data storage, remote communication, strain analysis and temperature analysis interfaces are also provided.

3. System Testing and Analysis

To verify sensing performance, a single-wavelength UW-FBG array with a wavelength of 1537 nm, reflectivity of 0.05% and spacing of 2 m was connected to channel 1 of the demodulation module. The positions of 400 grating points were calibrated, and the position and relative power distribution were obtained. In test mode, the demodulation frequency was 1 Hz. The measured wavelengths of 399 grating points were distributed between 1537.2959 nm and 1538.2973 nm. The spectrum of a single grating had a Gaussian distribution, with a full width at half maximum of 0.15 nm. The short-term wavelength stability was within 0.0003 nm and the long-term stability was below 2 pm.

The point at position 1 showed abnormal wavelength fluctuation. Combined with the spectrum, this was identified as a false grating caused by excessive reflection from the FC/APC end face and can be manually removed in the host software.

To further improve the resolution of the demodulation module, a multi-wavelength UW-FBG array was tested. The array had wavelengths of 1529 nm, 1541 nm and 1553 nm, a spacing of 0.5 m and a total length of 1335 m. At a demodulation frequency of 1 Hz, the demodulated wavelengths were near 1528.6430 nm, 1541.0089 nm and 1552.5672 nm, and the number of UW-FBGs was 2670. The single-grating spectrum remained Gaussian with a FWHM of 0.15 nm, short-term stability within 0.0003 nm and long-term stability below 2 pm, proving good measurement accuracy and stability for multi-wavelength arrays.

In multi-channel mode, cyclic acquisition was used to realize time-division demodulation of multiple channels. In a four-channel example, channels 1 and 2 were connected to single-wavelength gratings, while channels 3 and 4 were connected to multi-wavelength gratings. Each channel was calibrated to obtain grating position and relative power. The grating count, wavelength distribution and position information confirmed that the module also provides stable and accurate demodulation for multi-channel wavelength arrays.

To verify the working distance, a 10 km bare fiber was used as the lead fiber and connected to a UW-FBG array with a wavelength of 1541 nm, spacing of 0.5 m and total length of 436 m. At a demodulation frequency of 1 Hz, the demodulated wavelengths were distributed between 1541.0600 nm and 1541.1100 nm, and the number of UW-FBGs was 872. The single-grating spectrum was approximately Gaussian with a FWHM of 1.20 nm and slight distortion. Short-term wavelength stability was within 0.010 nm and long-term stability was below 25 pm. The demodulation error in long-distance arrays mainly came from the higher EDFA gain required at longer sensing distance; excessive launched power induced nonlinear effects and complex noise.

4. Conclusion

This paper proposes a modular multi-channel demodulation system based on UW-FBGs. The sensing principle and key parameters are analyzed. Low-level hardware is used to accurately locate UW-FBGs and process signals, enabling high-accuracy multi-channel time-division demodulation. The demodulation module consumes less than 13 W, measures 230 mm x 170 mm x 40 mm, provides a spatial resolution of 2 m, a single-channel sensing distance above 10 km and approximately 5,000 grating points. Test results show that the system offers high demodulation accuracy, stability and strong data-processing capability. It effectively solves the problems of massive data processing and transmission and meets the needs of future large-capacity sensing networks.

Translated Tables

Table 1. Tested grating sample parameters and measured results

Channel	Center wavelength (nm)	Spatial resolution (m)	Length (m)	Measured grating points	Measured wavelength (nm)
1	1535	2	694	347	1534.6141-1534.6149
2	1537	2	155	70	1537.1536-1537.1542
3	1529 / 1541 / 1553	0.5	10	10	near 1528.7537 / 1541.0814 / 1552.8408
4	1529 / 1541 / 1553	0.5	10	17	near 1528.7237 / 1541.0237 / 1552.6638

References

Reference entries are retained in the original citation form to avoid altering source bibliographic data.

- 万贤杰,江殿亮,徐军,易波.光纤智能测温度系统在电网上的运用[J].电子测量技术,2011,34(01):86-89.
- 苑立波,童维军,江山,杨远洪,孟洲,董永康,云江,何祖源,靳伟,刘统玉,邹琪琳,毕卫红.我国光纤传感技术发展路线图[J].光学学报,2022,42(01):9-42.
- STEPANOY K V, ZHIRNOV A A, CHERNUTSKY A O, KOSHELEY K I, PNEY A B, LOPUNOY A I, BUTOV O V. The Sensitivity Improvement Characterization of Distributed Strain Sensors Due to Weak Fiber Bragg Gratings[J]. Sensors,2020,20(22).
- WANG J, LIU Z C, YANG J H, ZHANG Z T. Research on Networking Algorithm of Distributed FBG Sensor Network, Mobile Information Systems,2021:7.
- WANG Y M, GONG J M, DONG B, WANG D Y, SHILLIG T J, WANG A B. A large serial time-division multiplexed fiber Bragg grating sensor network[J] Journal of Lightwave Technology, 2012, 30(17), 2751–2756.
- HAN P, LI Z Y, CHEN L, BAO X Y. A High-Speed Distributed Ultra-Weak FBG Sensing System With High Resolution[J]. IEEE Photonics Technology Letters, 2017, 29(15): 1249-1252.
- LIANG X, XIANG N, LI Z Y, ZHOU L, LIU Q, BAO X Y. Precision Dynamic Sensing With Ultra-Weak Fiber Bragg Grating Arrays by Wavelength to Frequency Transform [J]. Journal of Lightwave Technology, 2019, 37(14): 3526-3531.
- LI C L, TANG J Q, CHENG C, CAI L B, GUO H Y, YANG M H. Simultaneously distributed temperature and dynamic strain sensing based on a hybrid ultra-weak fiber grating array[J]. Optics Express,2020,28(23).
- GAO W J, LIU J X, GUO H Y, JIANG X, SUN S F, YU H H. Multi-Wavelength Ultra-Weak Fiber Bragg Grating Arrays for Long-Distance Quasi-Distributed Sensing [J]. Photonic Sensors, 2021,12(2):1-11.
- LOPEZ J H, SHLYAGIN M G, MARTINEZ-MANUEL R. Correlation-based multiplexing of spectral channels and fiber-optic sensors using unmodulated continuous-wave distributed feedback diode lasers[J]. Optics Letters,2022, 47(5):1210-1213
- GAN W B, LI S, LI Z Y, SUN L Z. Identification of Ground Intrusion in Underground Structures Based on Distributed Structural Vibration Detected by Ultra-Weak FBG Sensing Technology[J]. Sensors, 2019, 19(9): 2160- 2160.
- 陶鑫,江山,宋珂.基于弱光栅阵列低成本大长周界系统及其报警机制[J].中国激光,2020,47(04):225-233.
- LIU S P, SHI B, GU K, GU K, ZHANG C C, HE J H, WU J H, WEI G Q. Fiber-optic wireless sensor network using ultra-weak fiber Bragg gratings for vertical subsurface deformation monitoring[J]. Natural Hazards, 2021,109(3):1-17.
- 张晓飞,吕中虎,杨秀元,曾克,王晨辉.弱反射光栅滑坡监测系统的研究与应用[J/OL].电子测量技术,2022:1-6.
- MA L M, MA C, WANG Y M, WANG D Y, WANG A B. High-Speed Distributed Sensing Based on Ultra Weak FBGs and Chromatic Dispersion[J]. IEEE Photonics Technology Letters, 2016, 28(12): 1344-1347.
- XIAO L, NA X, LI Z Y, ZHOU L, ZHAO T, LIU X Y, BAO X Y. Precision Dynamic Sensing with Ultra-Weak Fiber Bragg Grating Arrays by Wavelength to Frequency Transform[J]. Journal of Lightwave Technology, 2019, 37(14): 3526-3531.
- LUO Z H, CHENG W S, ZENG S G, HE H L. Deformation detection of a double-clamped beam according to ultra-weak fiber Bragg grating[J]. Applied Optics, 2020, 59(31): 9765-9770.
- 桂鑫,李政颖,王洪海,王立新,郭会勇.基于大规模光栅阵列光纤的分布式传感技术及应用综述[J].应用科学学报, 2021, 39(05) : 747-776.
- LIU Y M, LIN Q S, LI W S, ZHANG S. Design of High-Performance Storage System Based on Zynq[J]. Scientific Journal of Intelligent Systems Research, 2021,3(3): 2664-9640.
- 柯宇锴,郑羽,刘宇,郭会勇,余海湖.全同弱光纤光栅阵列反射信号仿真计算与分析[J].光通信研究, 2015(04) : 39-41.
- WANG Y, GONG J M, WANG D Y, WANG D Y, DONG B, BI W H, WANG A B. A quasi-distributed sensing network with time-division-multiplexed fiber Bragg gratings[J]. IEEE Photonics Technology Letters, 2010, 23(2): 70-72.

作者简介

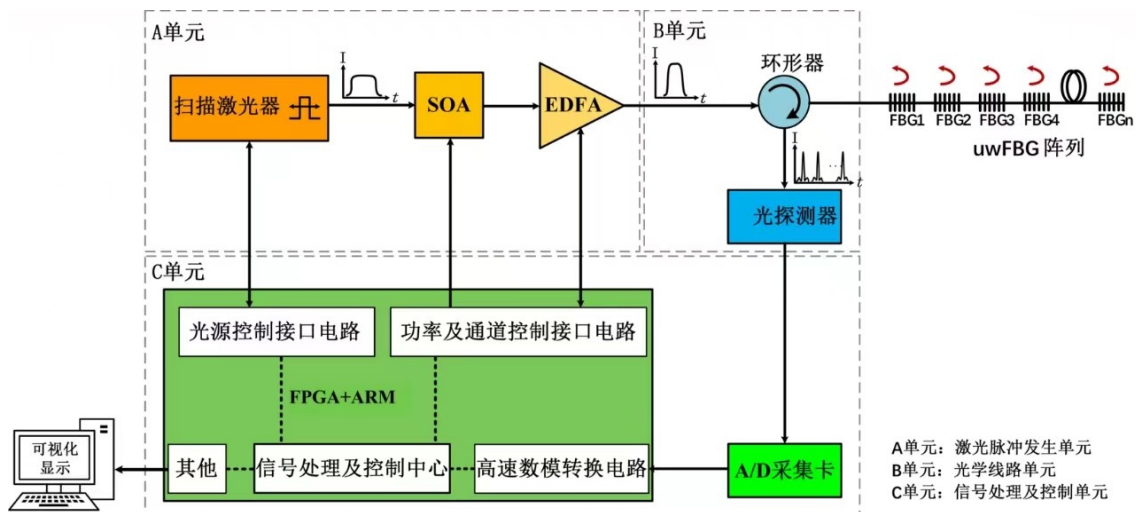
罗志会,工学博士,副教授,主要研究方向为先进光纤传感技术及其应用研究,光纤温度/应变分析仪、DAS系统的开发等。

E-mail : zhihui_luo@126.com

Retained Figures and Visual Materials

The original figures, screenshots, diagrams and experimental plots from the source manuscript are retained below in their original order for layout continuity. Captions in the translated body follow the source numbering where available.

Original visual material 1

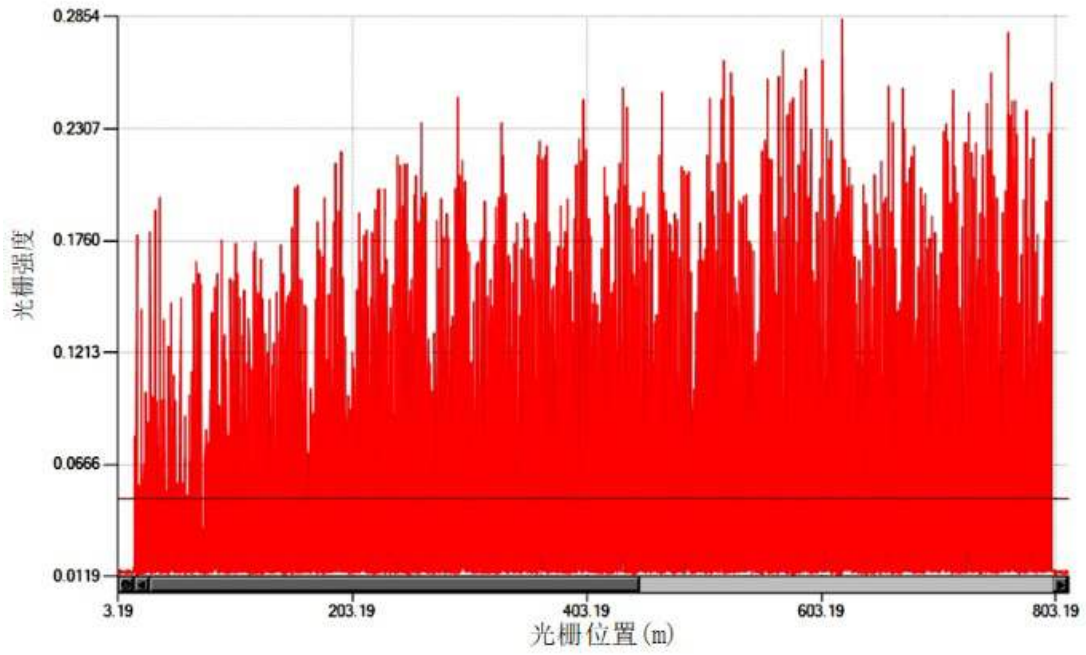


Original visual material 2

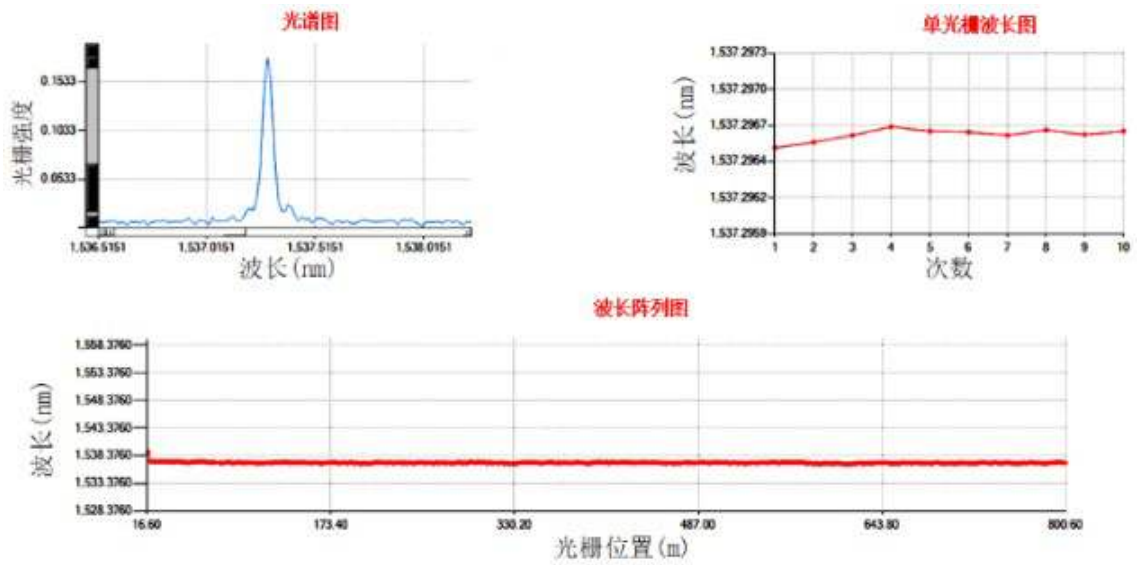


Original visual material 3

初始化波形图

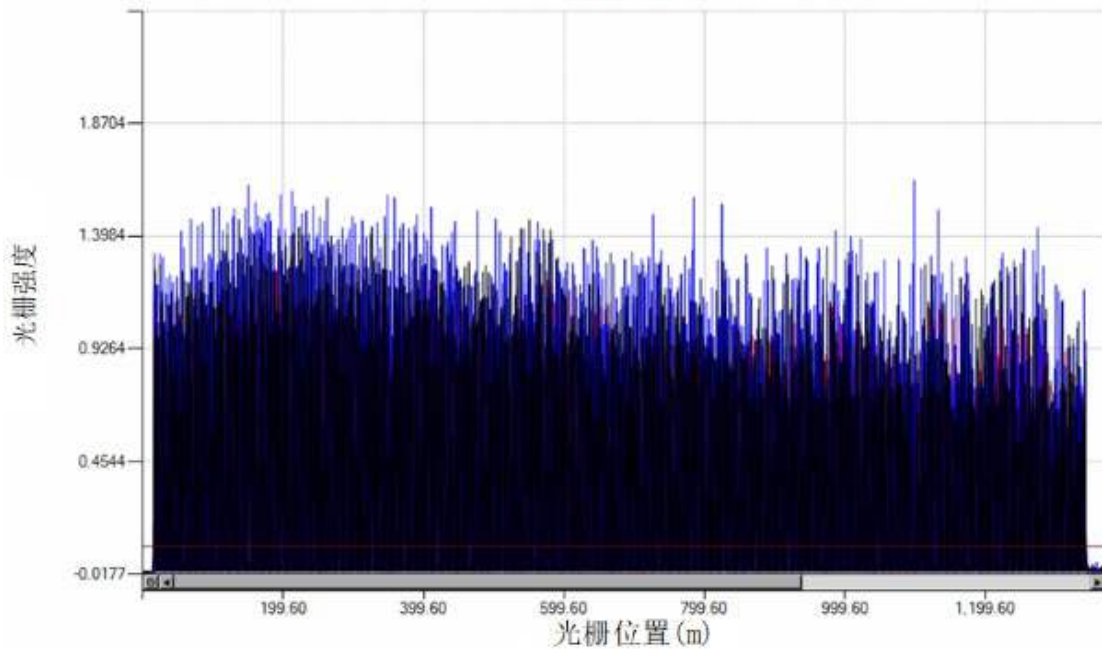


Original visual material 6

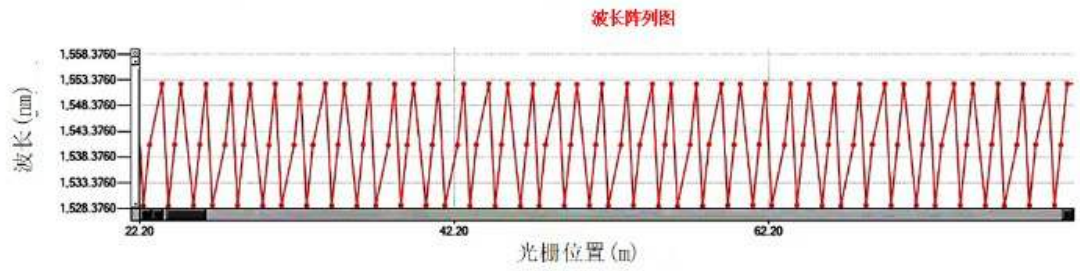
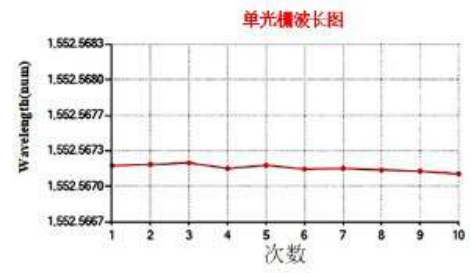
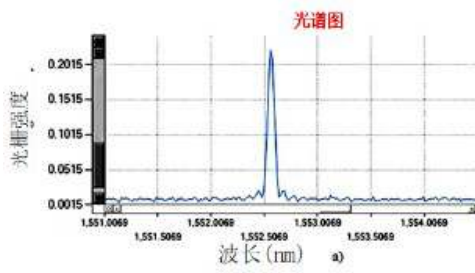


Original visual material 7

初始化波形图

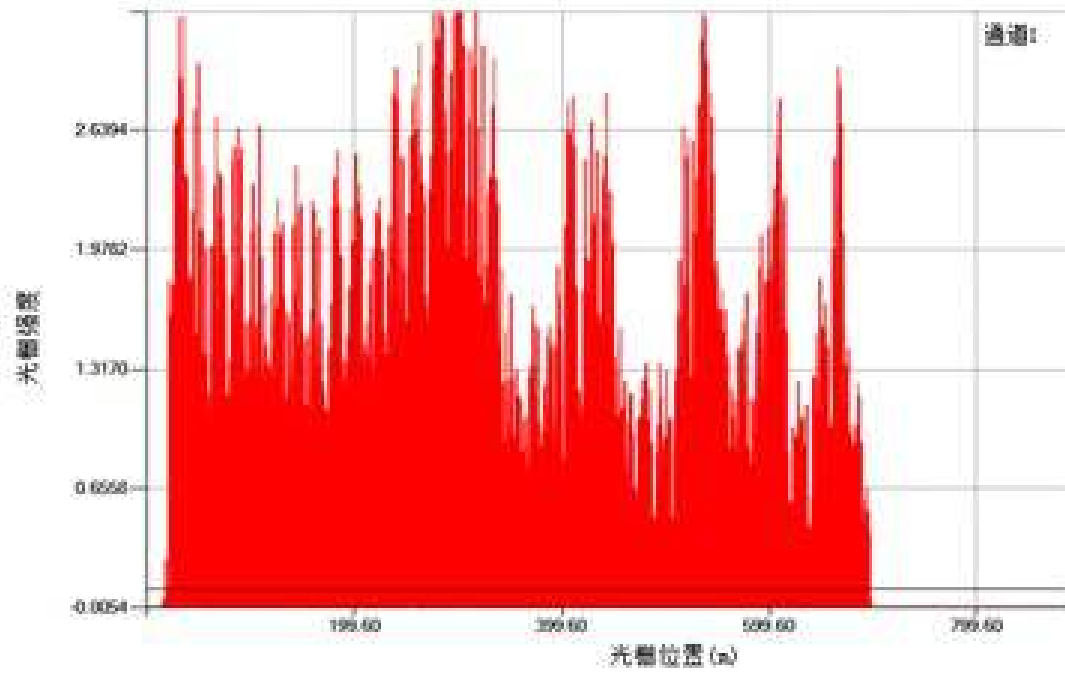


Original visual material 8

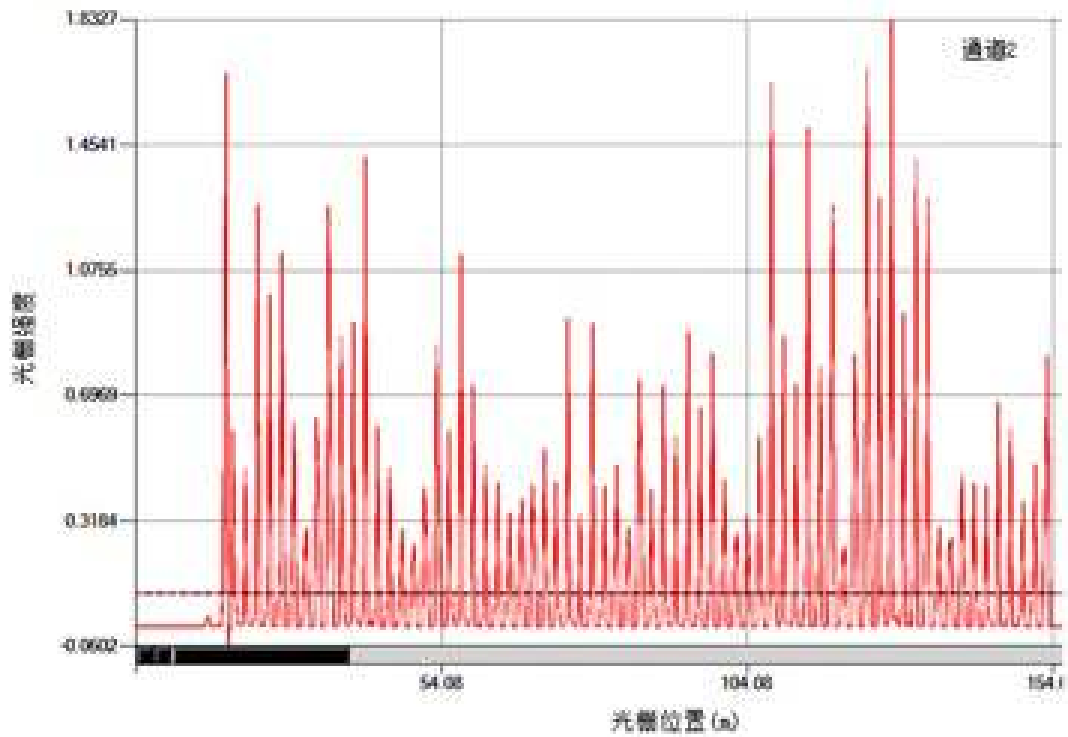


Original visual material 9

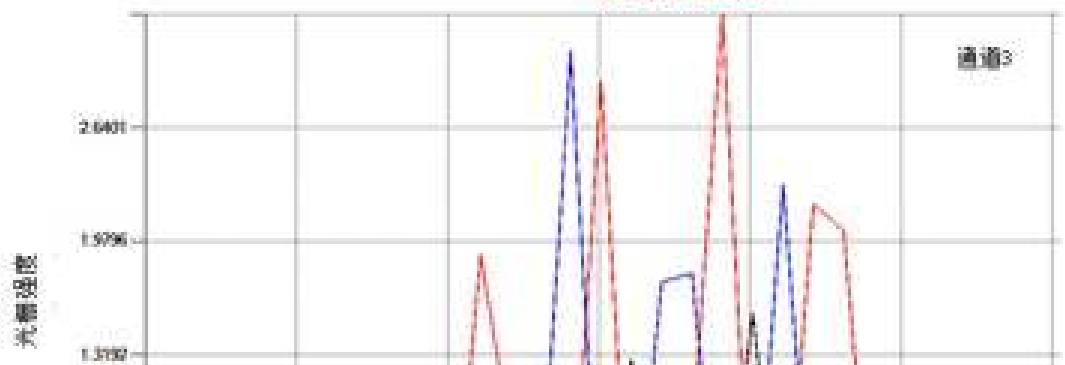
初始化波形图



初始化波形图

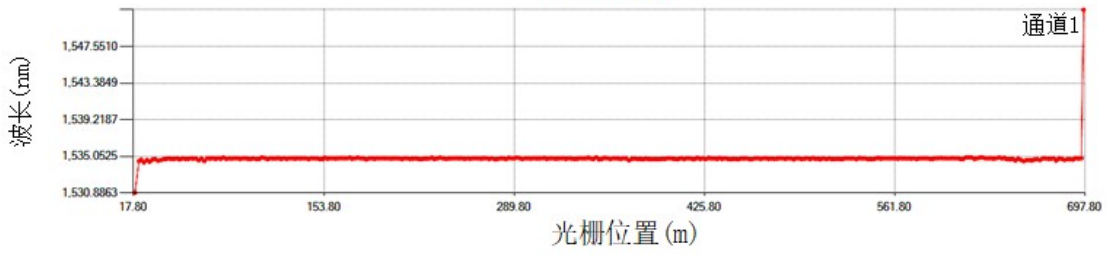


初始化波形图

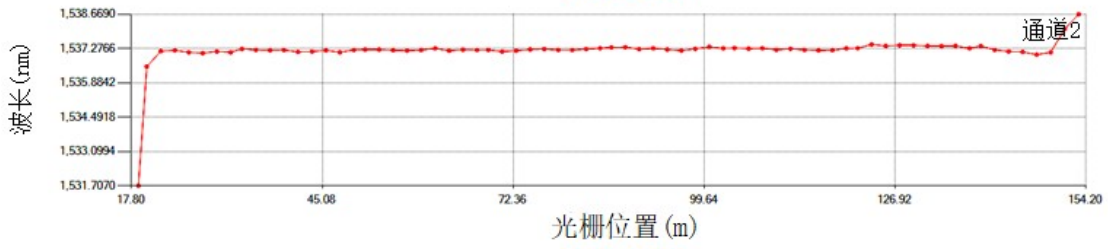


Original visual material 10

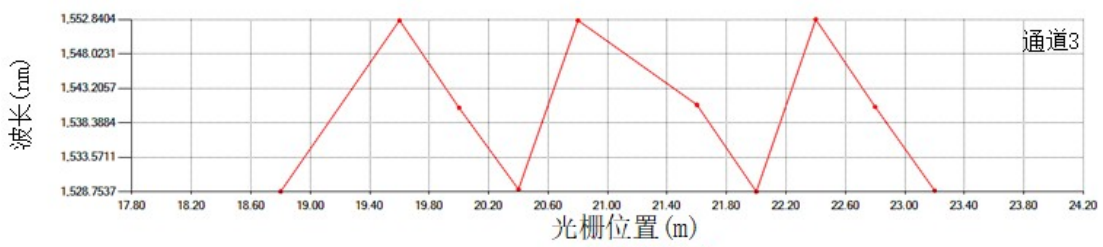
波长阵列图



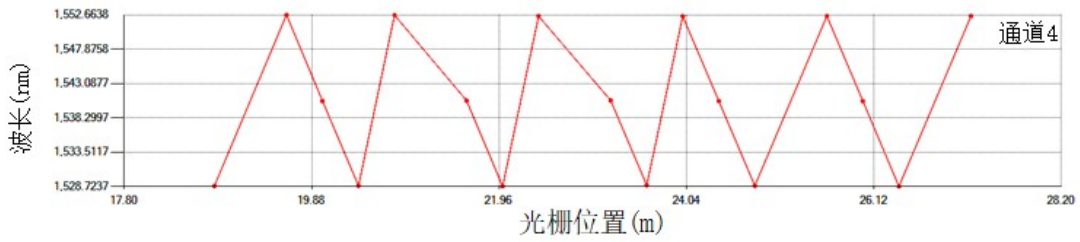
波长阵列图



波长阵列图

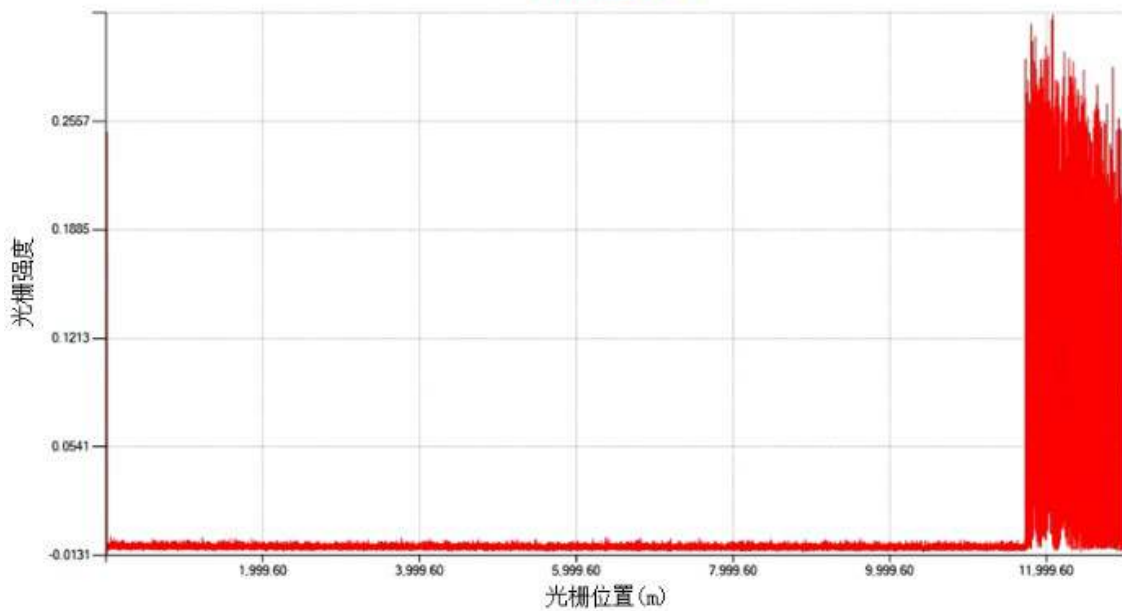


波长阵列图



Original visual material 11

初始化波形图



Original visual material 12

